Alternative Explanation of Stiffening in Cross-Linked Semiflexible Networks

P. R. Onck, T. Koeman, T. van Dillen, and E. van der Giessen

Micromechanics of Materials, Materials Science Centre, Nijenborgh 4, 9747 AG Groningen, The Netherlands

(Received 16 February 2005; published 18 October 2005)

Strain stiffening of filamentous protein networks is explored by means of a finite strain analysis of a two-dimensional network model of cross-linked semiflexible filaments. The results show that stiffening is caused by nonaffine network rearrangements that govern a transition from a bending-dominated response at small strains to a stretching-dominated response at large strains. Filament undulations, which are key in the existing explanation of stiffening, merely postpone the transition.

DOI: 10.1103/PhysRevLett.95.178102 PACS numbers: 87.16.Ka, 82.35.Lr, 87.15.La

There is a deep interest in the mechanical response of biological tissues and gels in view of the importance for biological functions such as cell motility and mechanotransduction. Many networklike biological tissues respond to deformation by exhibiting an increasing stiffness, i.e., ratio between change of stress and change of strain. This has been demonstrated by micropipette and microtwisting experiments [1] on individual cells and through rheological experiments on in-vitro gels of cytoskeletal filaments (actin, vimentin, keratin [2–6], and neuronal intermediate filaments [7]), as well as on fibrin [8,9]. These biological gels fall within the class of *semiflexible* polymers, which has also attracted much theoretical attention in the last decade [10–15]. However, these theoretical studies have primarily focused on the small-strain regime, tractable for analytical treatment.

In a simple conceptual view, a biopolymer network is an *interlinked* structure of *filaments*. Thus, stiffening can result from the response of the polymeric filaments between cross-links, from alterations in the network structure, or both. The current paradigm is that stiffening is primarily due to the longitudinal stiffening of the filaments themselves. This idea has been worked out in detail very recently by Storm *et al.* [16] by adopting the wormlike chain model for actin filaments in combination with the assumption that the network deforms in an affine manner, i.e., each filament is assumed to follow the overall deformation. The wormlike chain model is a well-documented description for the stretching of semiflexible polymers, where the longitudinal stiffness of undulated filaments is attributed primarily to bending fluctuations; the axial stiffness of the polymeric chain itself is much higher [10]. As the filament is stretched (at constant temperature), the amplitude of the transverse thermal undulations reduces and, as a consequence, the stiffness increases. In the limit that the filament is pulled straight, all subsequent axial deformation would have to originate from axial straining of the chain, but at an enormous energy cost. Given this description of individual filaments, Storm *et al.* [16] proceed by considering a network consisting of infinitely many filaments. Initially the filaments are randomly orientated, and as the sample is deformed the network is assumed to distort in an affine manner. The affine deformation assumption is well known in network models for rubber elasticity, and allows for a relatively simple description of the overall network response on the basis of the behavior of a single filament. The small-strain affine deformation assumption in two-dimensional networks of straight filaments has recently been studied in great detail by Head *et al.* [13,14] and Wilhelm and Frey [15], who conclude that network deformation is nonaffine for compliant, low-density networks and affine for stiff, high-density networks.

In this Letter we focus on the strain stiffening of networks that are nonaffine at small strains and demonstrate that stiffening lies in the network rather than in its constituents. We show that during deformation, the filaments rotate in the direction of straining, which induces a transition from a bending-dominated response to one that is controlled by stretching of aligned filaments. By comparing cross-linked networks with straight and undulated filaments, we show that filament reorientation is the dominant mechanism, while the undulations only postpone the onset of stiffening.

Our model is a two-dimensional network model of filaments in a periodic unit cell of dimensions $W \times W$. The network is generated by randomly placing filaments of length L at random orientations inside the cell, with proper account of periodicity. The filaments are elastic rods, characterized by a stretching stiffness μ (axial force [17] needed to induce a unit axial strain) and a bending stiffness κ (bending moment needed to induce a unit radius of curvature) [18]. The total free energy of the system consists of bending energy, $E_{\mathrm{bn}} = \sum \int_0^{L_c} \frac{1}{2}\kappa(\phi')^2 ds$, in addition to stretching energy $E_{\mathrm{ax}} = \sum \int_0^{L_c} \frac{1}{2}\mu(u')^2 ds$, where ϕ' is the curvature and u' the axial strain along the filament with contour length L_c, parametrized by s; the summations extend over all filaments. We choose an initial filament configuration consistent with a thermal distribution of transverse normal modes of the type $b_n \sin(n\pi x/L)$, where the ampitudes b_n follow a Gaussian distribution (cf. [19]) with standard deviation $\sqrt{2/(l_p L)}(L/n\pi)^2$. The persistence length l_p, i.e., the distance over which the filaments appear straight, is expressed as $l_p \propto \kappa/(k_B T)$ in terms of the

bending stiffness κ of the filaments, Boltzmann's constant k_B and temperature T. We use the first 10 normal modes to generate the initial geometry of the filaments and treat l_p as an independent quantity. During mechanical loading, thermal effects are no longer taken into account.

Points where filaments overlap are considered to be cross-links, similar to the procedure used by Head *et al.* [13,14] and Wilhelm and Frey [15]. The networks generated by this procedure are taken as the initial, stress-free configuration. In the calculations, the cross-links are assumed to be stiff, so that both displacement and rotation of the two filaments at the cross-link point remain the same. It should be noted that, in accordance with previously developed models [13–15], the cross-links are permanent, so that dynamic effects, such as those caused by dynamic cross-link alterations, are neglected. The density of the network is characterized by the line density ρ, i.e., the total length of filaments in the unit cell divided by the cell area, W^2. For networks with straight filaments ($l_p/L \to \infty$), the average distance between cross-links, l_c, is inversely proportional to ρ through $l_c = \pi/\rho$ [20]. We consider networks of different densities above the rigidity percolation threshold [15] but below the lower bound, $L/\lambda = L/l_c(\sqrt{\kappa/\mu}/l_c)^{1/3} \approx 20$, for which affine behavior is expected at small strains [13,14].

For the numerical study we use the finite element method, discretizing each filament with 10 equal-sized Euler-Bernoulli beam elements accounting for stretching and bending. Geometry changes are accounted for by an updated Lagrangian finite strain formulation. All filaments are perfectly bonded to rigid top and bottom plates, with the top plate displaced horizontally relative to the bottom plate over a distance ΓW, corresponding to an applied shear strain Γ. The macroscopic shear stress τ is calculated from the total horizontal reaction force at the top, divided by W. Convergence studies ensured that the cell size W does not affect the results.

The parameters governing the system are τ, Γ, μ, κ, L, ρ, and l_p. We choose to present the results through the following dimensionless parameters: $\bar{\tau} = \tau L/\mu$, Γ, $\bar{\rho} = \rho L$, $\bar{l}_p = l_p/L$, and $\bar{l}_b = \sqrt{\kappa/(\mu L^2)}$. Note that $\bar{l}_b$ is a measure for the flexibility of the filaments, which reduces to the slenderness ratio (thickness over length) for isotropic elastic rods, and $\bar{l}_p$ sets the initial shape of the filaments.

In a first set of calculations we take $\bar{l}_b = 2.3 \times 10^{-4}$ and $\mu/L = 1.6$ MPa (representative for actin microfilaments [21]) with a density of $\bar{\rho} = 13$, which is well above the rigidity percolation threshold of $\bar{\rho} = 5.7$ [15]. The persistence length is taken to be much larger than the filament length ($\bar{l}_p \gg 1$), corresponding to straight filaments. Figure 1 shows the stress-strain response (averaged over ten different random realizations). Three regimes can be identified: a regime with a relatively low stiffness $d\bar{\tau}/d\Gamma$, a transition regime, and a high-stiffness regime. Figure 2 shows three snapshots of the network geometry at $\Gamma = 0$, 0.08, and 0.24 for a typical realization close to the average response (see the solid squares in Fig. 1). Comparison of Fig. 2(b) with Fig. 2(a) reveals that many initially straight filaments have deformed by bending, which corresponds to the characteristic low stiffness at small strain levels for these densities [13–15]. Subsequently, during the transition regime, percolations of stretched filaments appear that connect the top and bottom of the cell along a $\sim 45°$ direction, Fig. 2(c). These filaments are loaded in axial tension, resulting in a higher overall stiffness. Thus, Figs. 2(b) and 2(c) demonstrate the transition from a bending-dominated regime at small strains (total mechanical energy of the systems primarily consists of bending energy $E_{ax}/E_{bn} = 0.0087$) to a stretching-dominated regime at higher strain levels (total energy dominated by the axial stretching energy $E_{ax}/E_{bn} = 9.5$).

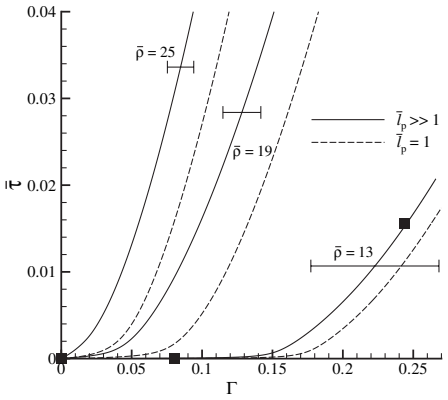

FIG. 1. Average stress ($\bar{\tau}$) versus strain (Γ) response for networks with $\bar{l}_b = 2.3 \times 10^{-4}$ and $\mu/L = 1.6$ MPa at three different densities $\bar{\rho}$ and for straight ($\bar{l}_p \gg 1$) and undulated ($\bar{l}_p = 1$) filaments. The error bars have a length of 2 times the standard deviation in strain at a given Γ for ten different realizations at each density. The squares correspond to three instances during deformation for which the network geometry is shown in Fig. 2.

The stress-strain response for two higher densities, $\bar{\rho} = 19$ and 25, is included in Fig. 1. The standard deviation in strain from ten realizations is approximately independent of the stress value for a given density. The scatter in strain, defined as the ratio between the standard deviation and the average, is independent of the density and has a value of approximately 0.2. Figure 1 shows that a certain stress level is achieved at smaller strains in case the network is denser. The network thus gets stiffer with increasing density, while the transition from bending to stretching becomes less abrupt and occurs at smaller strain levels.

Next, the effect of filament undulations is investigated. The same parameters are used as before, but now we use $\bar{l}_p = 1$, corresponding to a filament length of order 10 μm, as found in many in-vitro experiments [21]. Changing the persistence length from $l_p \gg L$ to $l_p = L$ is physically similar to increasing the temperature from 0 K to 293 K before cross-linking and loading the network instantaneously. Figure 3 depicts the initial geometry for a network where the initial filaments' end-to-end vectors have the

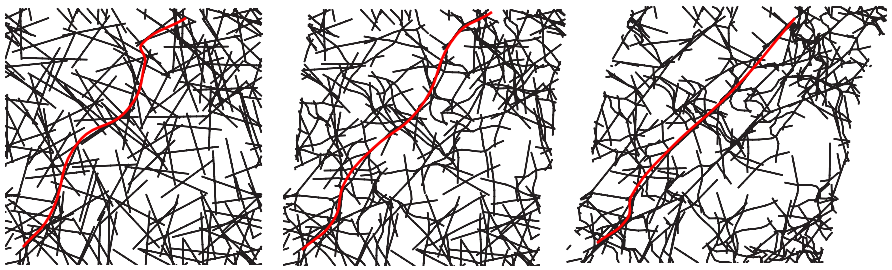

FIG. 2. (a) Initial, $\Gamma = 0$; (b) intermediate, $\Gamma = 0.08$, and (c) large strain, $\Gamma = 0.24$, network configurations for a typical $\bar{\rho} = 13$ realization close to the average response shown in Fig. 1 (squares). For an animation see Ref. [25].

same location and orientation as shown in Fig. 2(a). The stress-strain results included in Fig. 1 (dashed lines) show that the undulations do not change the shape of the overall stress-strain curve, but merely delay the transition from bending to stretching. The associated ''delay'' strain at an applied strain level of $\Gamma = 0.25$ is 0.018, 0.029, and 0.024 for $\bar{\rho} = 13$, 19, and 25, respectively. Similar values were found for densities up to 38. Clearly, only a small fraction of the total strain is due to the presence of filament undulations.

To make connection with the small-strain study by Head *et al.* [13], we monitor the degree of affinity of the network during straining to large deformations. For this purpose, we define the deviation from affine behavior, ΔA, as

$$\Delta A = \frac{1}{n} \sum_{k=1}^{n} \frac{\|\Delta \mathbf{r}^{(k)} - \Delta \mathbf{r}^{(k)}_{\text{aff}}\|}{\Delta\Gamma \|\mathbf{r}^{(k)}\|}, \qquad (1)$$

where $\|\mathbf{r}\|^2 = \mathbf{r} \cdot \mathbf{r}$, n is the number of cross-links, and $\mathbf{r}^{(k)}$ is the current position vector of cross-link k. $\Delta \mathbf{r}^{(k)}$ is the increment in the position of cross-link k during a shear increment $\Delta\Gamma$ in the simulations, while $\Delta \mathbf{r}^{(k)}_{\text{aff}}$ is the corresponding value were the deformation affine. Figure 4 shows the evolution of ΔA as a function of Γ for the cases shown in Fig. 1. It is observed that the deformation is not affine at small strains, in accordance with Refs. [13–15], while the deformation becomes increasingly affine ($\Delta A \rightarrow 0$) with increasing strain. By comparing Fig. 4 with Fig. 1, we find that in the transition from the bending to the stretching regime, ΔA increases significantly, indicating a reorientation of the filaments. The peak in the ΔA-Γ curve occurs for both straight and undulated filaments in the transition regime. This is another indication of the fact that filament undulations do not change the nature of network deformation, but merely enhance the strain value at which stretching sets in. Once stretching has set in, the deformation becomes more and more affine.

To study the influence of the filament properties, the calculations are repeated, but with a larger bending and stretching stiffness, $\bar{l}_b = 8.3 \times 10^{-4}$ and $\mu/L = 8$ MPa (representative for microtubuli [22]). Note that the bending stiffness increases by a factor of 65, while the stretching stiffness becomes 5 times larger. Because of the enhanced bending stiffness, the persistence length at the high temperature increases from $\bar{l}_p = 1$ to 65 so that the filaments are almost straight (in accordance with experimental observations on microtubuli [21]). Figure 5 shows the instantaneous shear stiffness, $\bar{G} = d\bar{\tau}/d\Gamma$ [23], as a function of shear strain Γ for the two different values of $\bar{l}_b$ (and reference stress μ/L). It can be observed that for the flexible filaments ($\bar{l}_b = 2.3 \times 10^{-4}$) the transition from the low-stiffness to the high-stiffness regime shifts to lower strains with increasing density, consistent with Figs. 1 and 4. For densities higher than $\bar{\rho} = 25$, the transition from bending to stretching is no longer accompanied by severe filament reorientations that cause a peak in ΔA (see Fig. 4), but progresses more smoothly. At higher densities of either

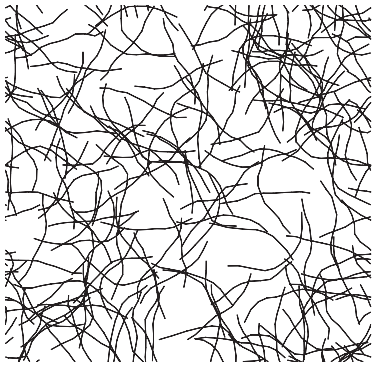

FIG. 3. Initial conformation of a $\bar{\rho} = 13$ network with undulated filaments corresponding to $\bar{l}_p = 1$.

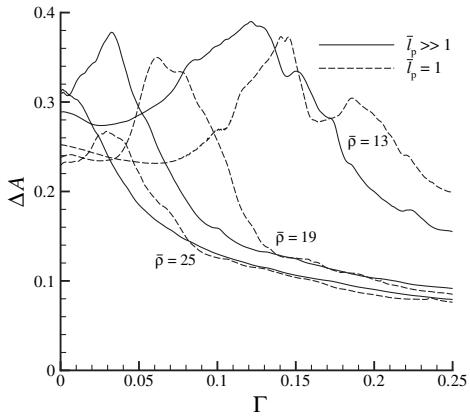

FIG. 4. The deviation from affine behavior, ΔA, as a function of strain, Γ, for $\bar{l}_b = 2.3 \times 10^{-4}$ and $\mu/L = 1.6$ MPa, at three different densities and for straight ($\bar{l}_p \gg 1$) and undulated ($\bar{l}_p = 1$) filaments.

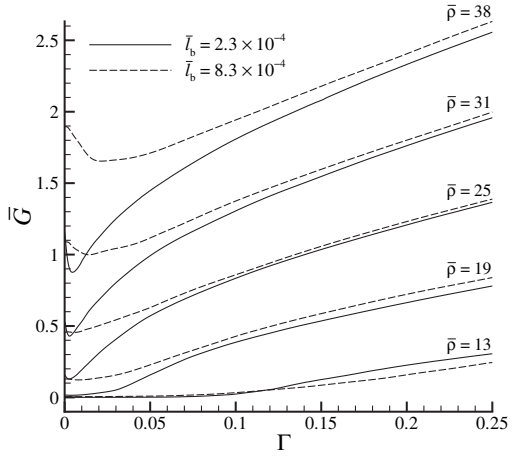

FIG. 5. Shear stiffness as a function of strain for networks with straight filaments having $\bar{l}_b = 2.3 \times 10^{-4}$ or 8.3×10^{-4}.

floppy or stiff filaments, the stiffness first decreases with strain at small-strain levels. This is caused by buckling of filaments oriented at 135° away from the horizontal axis (positive to the right in Fig. 2), which are loaded primarily in compression. Figure 5 also shows that at small strains the overall stiffness for the floppy filaments is much lower than that of the stiffer filaments, but converges to the same value at larger strains. This reflects that bending is the dominant deformation mode in the low-stiffness regime at small strains, while filament stretching governed by μ dominates at large strains.

The level of affinity at small strains can be conveniently characterized by the length scale $\lambda = l_c(l_c/l_b)^{1/3}$ [14]: nonaffine behavior is predicted for low L/λ and affine behavior for high L/λ. The networks investigated in this Letter are nonaffine with L/λ ranging between 0.4 and 2.6. Although a comparison of the two-dimensional results with real three-dimensional network behavior should be made with great care and can only be qualitative, an estimate of L/λ at physiological relevant conditions can be obtained. The mesh size ($\approx l_c$) of actin networks, for instance, ranges from 0.2 to 2 μm for densities between 0.1 and 3 mg/ml [24]. With $l_b = 2.3$ nm and $L = 10$ μm [21] this leads to $L/\lambda = 0.5$ and $L/\lambda = 10$ for the low and high densities, respectively. The mechanism of strain-stiffening proposed in this Letter is therefore expected to be active in actin networks for densities up to 1 mg/ml. For biopolymer networks consisting of filaments with lower bending stiffnesses than actin, such as fibrin and intermediate filaments, the current stiffening mechanism will be active up to higher densities. Future work is aimed at extending the current two-dimensional model to three dimensions which will enable us to compare the results with available experimental data and previously developed models [14,16].

This study leads to the following conclusions. Stiffening of nonaffine, cross-linked semiflexible networks is caused by the transition of a bending-dominated response at small strains to a stretching-dominated response at large strains. This transition is mediated by network rearrangements. Filament undulations only have a minor effect; they merely postpone the transition from bending to stretching.

[1] N. Wang and D. E. Ingber, Biochem. Cell Biol. **73**, 327 (1995).
[2] M. L. Gardel, J. H. Shin, F. C. MacKintosh, L. Mahadevan, P. Matsudaira, and D. A. Weitz, Science **304**, 1301 (2004).
[3] J. Xu, Y. Tseng, and D. Wirtz, J. Biol. Chem. **275**, 35 886 (2000).
[4] Y. Tseng, K. M. An, O. Esue, and D. Wirtz, J. Biol. Chem. **279**, 1819 (2004).
[5] P. A. Janmey, U. Euteneuer, P. Traub, and M. Schliwa, J. Cell Biol. **113**, 155 (1991).
[6] L. Ma, J. Xu, P. A. Coulombe, and D. J. Wirtz, J. Biol. Chem. **274**, 19 145 (1999).
[7] J. F. Leterrier, J. Käs, J. Hartwig, R. Vegners, and P. A. Janmey, J. Biol. Chem. **271**, 15 687 (1996).
[8] M. D. Bale and J. D. Ferry, Thromb. Res. **52**, 565 (1988).
[9] P. A. Janmey, E. Amis, and J. Ferry, J. Rheol. (N.Y.) **27**, 135 (1983).
[10] F. C. MacKintosh, J. Käs, and P. A. Janmey, Phys. Rev. Lett. **75**, 4425 (1995).
[11] H. Isambert and A. C. Maggs, Macromolecules **29**, 1036 (1996).
[12] D. C. Morse, Phys. Rev. E **58**, R1237 (1998).
[13] D. A. Head, A. J. Levine, and F. C. MacKintosh, Phys. Rev. E **68**, 061907 (2003).
[14] D. A. Head, A. J. Levine, and F. C. MacKintosh, Phys. Rev. Lett. **91**, 108102 (2003).
[15] J. Wilhelm and E. Frey, Phys. Rev. Lett. **91**, 108103 (2003).
[16] C. Storm, J. J. Pastore, F. C. MacKintosh, T. C. Lubensky, and P. A. Janmey, Nature (London) **435**, 191 (2005).
[17] All quantities with dimension force are computed per unit out-of-plane thickness.
[18] For isotropic elastic rods, κ and μ are related through their cross-sectional geometry, but are treated here as independent.
[19] J. Käs, H. Strey, J. X. Tang, D. Finger, R. Ezzel, E. Sackmann, and P. A. Janmey, Biophys. J. **70**, 609 (1996).
[20] G. Pike and C. Seager, Phys. Rev. B **10**, 1421 (1974).
[21] J. Howard, *Mechanics of Motor Proteins and the Cytoskeleton* (Sinauer Associates, Inc., Sunderland, Massachusetts, 2001).
[22] Consider a microtubule (MT) having an inner radius of 8 nm and an outer radius of 12 nm. If we compare the stretching and bending stiffness with that of an actin microfilament (MF), represented by a solid rod of radius 4 nm, it follows that $\mu_{MT}/\mu_{MF} = 5$, $\kappa_{MT}/\kappa_{MF} = 65$.
[23] For nonlinear stress-strain behavior, the incremental stiffness $d(\text{stress})/d(\text{strain})$ should be used instead of *stress/strain*.
[24] C. F. Schmidt, M. Barmann, G. Isenberg, and E. Sackmann, Macromolecules **22**, 3638 (1989).
[25] See EPAPS Document No. E-PRLTAO-95-022544 for an animation of the network deformation shown in Fig. 2. This document can be reached via a direct link in the online article's HTML reference section or via the EPAPS homepage (http://www.aip.org/pubservs/epaps.html).